# Novel Polarization Interference Filters For Wide Spectral Tuning of an Optical Null

Hugh J. Masterson and Jay. E. Stockley
Boulder Nonlinear Systems, 450 Courtney Way, Lafayette Colorado 80026

## ABSTRACT

Novel tunable polarization interference filters (PIF) employing active liquid crystal devices are presented, and the principles of operation are described. Filter designs are presented based on a requirement for tunable nulls in the visible and near infrared spectral regions of high optical density, for protection from intense electromagnetic radiation outside of the spectral range of interest which can saturate an imaging or sensor system.. Two types of PIFs are presented with their modeled results and device performances. Analog filters in a generalized Lyot-Ohmann geometry are presented which are capable of tuning an optical null through 260 nm, by employing a single active device per filter stage. Binary filters are also presented which can switch between two complimentary and non-overlapping spectral states. Both types of filter can operate in a "normally on" state with a broadband "white light" throughput.

**Keywords:**Tunable polarization interference filters, liquid crystal devices, wide spectral tuning, high optical density.

## 1 INTRODUCTION

In the past three decades CCD camera and night vision technology have revolutionized the ability to image low light scenes. Imaging and sensor technology operates over a broadband spectrum covering the visible to near infrared and is thus susceptible to saturation from any relatively intense light source within this region. The provision of some tunable filter means to block out an unwanted portion of the visible to near infrared (NIR) spectral region is highly desirable for inclusion in the general imaging technology arsenal. A tunable filter capable of moving a high optical density (OD) absorption band to a desired location within the detection band of silicon would provide an agility for imaging and sensor systems which would allow them to operate with improved performance across a wide range of technologies. In addition to protection for unwanted intense radiation, the proposed technology would offer discrimination between different spectral signatures which would be useful for multispectral imaging in remote sensing, or in pattern recognition where spectral information is important. Night vision technology would also benefit from this addition, in circumstances where unwanted visible radiation threatened to obscure the image field.

Present tunable filter technology is often limited to rotating filter wheels or similar mechanical devices with moving parts where aperture sizes suitable for imaging are required, such as in hyperspectral or multispectral imaging. Technologies such as the acousto-optic tunable filter offer very narrow linewidths and high throughput, but the former feature in conjunction with the narrow field of view (FOV) make them unsuitable for broadband imaging. The preferred solution for tunable filter development in the present context is to use liquid crystal (LC) based polarization interference filters (PIFs)[1]. LC tunable filters have been proposed and demonstrated[2], mainly using the Lyot-Ohmann filter geometry[3,4] and employing zero-twist nematic liquid crystal voltage controllable waveplates[5]. However, these filters, although successfully tuning across a desired spectral band are typically "passband" rather than "stopband" oriented in that they focus on transmitting a desired spectral region for applications such as RGB color separation, where even significant leakage in the stopband is not problematic for visual color perception. In addition, typical tunable color filters employing nematic liquid crystals suffer from poor field of view and are limited by a slow (~100 ms) response time.

In the present report we present a series of tunable PIFs employing primarily smectic C* Ferroelectric liquid crystal (FLC) rotatable waveplates[6] as the active elements with the focus on achieving high OD tunable or switchable stopbands. Because of the high (ms) switching speeds of the smectic C* devices, the filters demonstrated can operate in tunable stopband mode, or in their "normally on" state where they can be rapidly dithered at video frame rates between

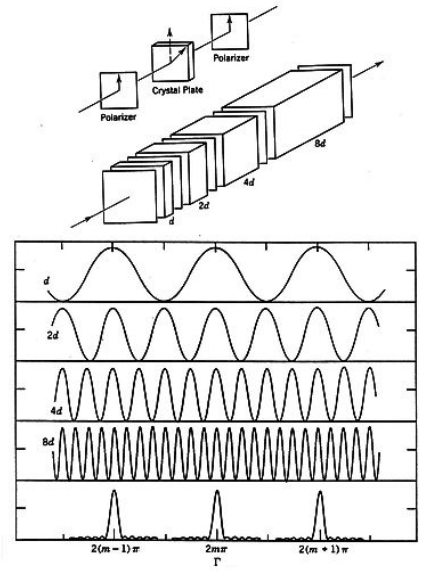


**Figure 1** A classic 4 stage Lyot-Ohmann filter with characteristic transmission spectra[4]

complimentary spectral state to give a perceived "white light" broadband throughput. In addition they offer improved FOV performance over their nematic based counterparts. Two different types of approaches are used to block a desired wavelength region; an analog filter approach and a binary filter approach. The former filters can be tuned continuously across the visible or NIR spectral regions and the latter can be switched between complimentary non-overlapping spectral states. Both types of filter are polarization interference based and can be considered as in terms of generalized Solc or Lyot-Ohmann filter geometries. The analog filter principle is demonstrated with broadband low order devices to achieve maximum spectral tuning width and deep nulls although the principle can be extended to higher order multistage devices. The filters presented are compared with modeled results using a Windows based 4x4 Mueller matrix software package which uses real polarizer and retarder material data in the calculations.

## 2 FILTER DESIGN

### 2.1 Analog Filter Design

The analog filters presented are constructed on the principle of the Lyot-Ohmann filter[2,3]. In this well known design, filter sections consisting of a pair of polarizers with parallel axes and a birefringent element at 45º to the polarization direction are cascaded together. In the classical design scheme, the optical thickness of the birefringent elements increases geometrically in a 1:2:4.. ratio, however, other design schemes are also possible and in this sense we refer to the Lyot-Ohmann filter in a general sense. The classical filter has a $sinc^2$ transmission function and exhibits a transmission peak at the design wavelength with oscillating sidebands, as shown in Figure 1. In the present context the sidebands are undesirable and the filter geometries were adjusted to eliminate these and bring the sideband energy into the central peak. One or two stage filters were designed and investigated for simplicity, with the principles being extendable to multistage devices. Tuning is achieved by appropriately varying the phase retardation in each stage while keeping the necessary filter geometry.

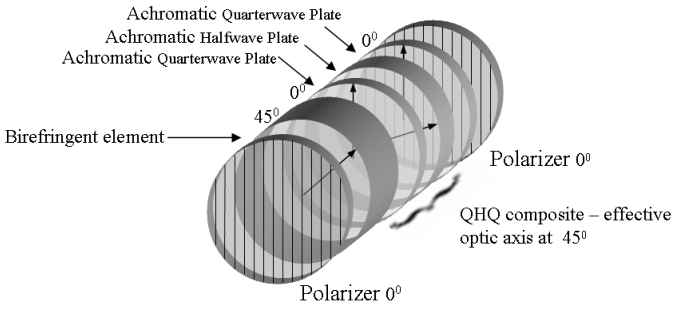


**Figure 2** Basic analog tuning configuration with an active FLC device employed to switch out different wavelength nulls as described in the text.

Unlike nematic LC devices which can act directly as voltage controlled phase modulators by rotating the optic axis perpendicularly to the plane of the cell, smectic FLC devices, which have an in plane optic axis must be coupled with additional elements if they are to function as phase modulators. Fortunately this can be achieved by means of the quarterwave-halfwave-quarterwave (QHQ) cell described by Title et al[7] which is the basis of the tuning mechanism of the analog filters reported here. This arrangement of retarding elements is a specific solution of the case of three birefringent plates, the first and last having identical retardations and parallel optic axes (fast axes) and the central element having variable orientation. This was shown by Pancharatnam[8] to be equivalent to a single element of retardation δ, possessing a optic axis inclined at an angle θ to the optic axes of the identical outermost plates. Here δ and θ are given by

$$\cos(\delta/2) = \cos 2\delta_1 \cos\delta_2 - \sin 2\delta_1 \sin\delta_2 \cos 2\rho \tag{1}$$

and

$$\cot 2\theta = \mathrm{cosec}\, 2\rho(\sin 2\delta_1 \cot\delta_2 + \cos 2\delta_1 \cos 2\rho) \tag{2}$$

where $2\delta_1$ is the retardance of the first and last plates, $2\delta_2$ is that of the central plate, and ρ is the angle between the optic axes of the central plate and the other two. If the outermost elements are chosen with half the optical thickness of the central element then at a wavelength $\lambda_0$, halfwave for the central element, the combination will behave as a QHQ cell. In this case

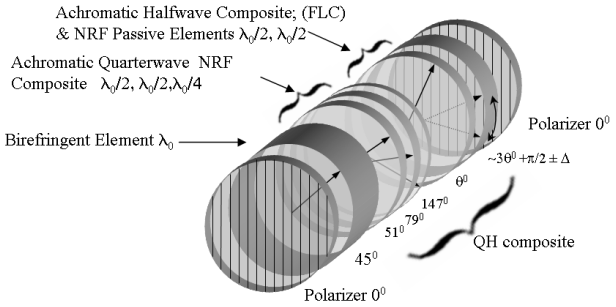


**Figure 3** Illustration of a basic analog tuning stage. The FLC device tunes about the angle $3\theta+\pi/2$ by $\pm\Delta$.

$$\delta = -4\rho \quad (\text{modulo } 2\pi) \tag{3}$$

and

$$\cot 2\theta = 0$$

so that the effective optic axis of the QHQ cell is always at 45º to the optic axes of the outer quarterwave plates. Here the retardation is linearly proportional to the angular position of the optic axis of the halfwave plate and a total analog rotation of $\pi/2$ of the halfwave plate optic axis produces a $2\pi$ change in the retardation.

Since the present application involves spectral tuning across a band of wavelengths the QHQ cell must operate everywhere in this region. This requires that the quarterwave and halfwave elements be achromatic in the tuning range. An achromatic QHQ cell of this type can be used for achromatic tuning of the retardation of a birefringent element, and when the complete assembly is placed between parallel polarizers as shown in Figure 2 with the optic axis at 45° to the polarization axes, the optical null may be tuned across the spectral band by varying $\delta$ as described.

A more in depth analysis of the QHQ modulator[9] reveals that in a single tuning stage such as shown in Figure 2, the last quarterwave element may be dispensed with without affecting the wavelength dependent transmission function. In fact this quarterwave-halfwave (QH) structure is conceptually easier to understand as a spectral tuning device. Briefly, the output of the birefringent element consists of a multitude of wavelength dependent elliptical polarizations. The quarterwave analyzer transforms these elliptical polarizations into linear polarizations with wavelength dependent angular orientation and the rotatable halfwave plate tunes the peak or null across the wavelength band.

The QH structure described above forms the tuning capability of the analog filters presented. Passive quarterwave elements are fabricated from a threefold stack of NRF retarder layers from Nitto Denko Inc based on the model by Pancharatnam[6] which combines two halfwave plates and an a quarterwave plate at $\lambda_0$, at appropriate angles with respect to the input plane of polarization. The output light has undergone a $\lambda/4$ retardation and is roughly circular over a broad wavelength range containing $\lambda_0$. With a center wavelength of 589 nm, the above scheme exhibits achromatic quarterwave behavior from 400nm to 780nm. A similar element can be constructed for the NIR spectral region of 700nm to 1000 nm.

The achromatic halfwave component of the QH cell is again achromatic over a finite wavelength span and must again be constructed from elements oriented in the appropriate manner. The halfwave plate arrangement is loosely based on the design of Koester[10] employing two halfwave retarder elements at the design wavelength and oriented with slow (or fast) axes at $\theta^o/4$ and $3\theta^o/4$ to the plane of the input polarization. It is noted that the standard operation of the Koester halfwave plate requires that both elements be tunable to maintain the correct angular ratio so that two FLC devices were thought to be necessary initially. However, it was found through modeling efforts that the first element could remain static while still maintaining a large tuning width by varying the optic axis orientation of the second element, which in this case is an FLC cell. Furthermore, it was found that centering the second element at approximately $3\theta+\pi/2$, yielded superior performance in terms of null optical density. Tuning of the FLC cell optic axis $\pm \Delta^0$ about its midpoint location therefore, controlled the spectral output of the filter. A new experimental liquid crystal compound with an 80º double tilt angle enabled the fabrication of filters with a 260 nm tuning range using a single active element in a filter stage. The FLC device is capable of analog voltage control of the LC director orientation despite being confined in the surface stabilized model [6]. To the authors knowledge, this spectral tuning width has not been achieved previously with smectic LC controlled tunable filters.

The actual orientation of active and passive elements to achieve optimal performance varied from filter to filter and was found through filter modeling, taking into account the dispersive behavior of the FLC and passive retarder elements.

Figure 3 shows the basic structure of the practical analog filter stage. Constructed devices usually required more elements than shown in Figure 3, since individual passive elements of the quarterwave of halfwave section were often constructed from more than one sheet of NRF material with crossed or parallel fast axes to give an additive or subtractive result to meet the design wavelength. This process could be simplified by acquiring single NRF layers for the required wavelength. These subcomponents were themselves adjusted in relative angular orientation according to modeling results to achieve further optimization. Optimizing the null OD by adjusting these angles was in some cases at the cost of a reduction in transmission in the passbands.

For initially investigation these tunable filters it was decided to achieve the maximum possible tuning angle per stage to exploit the angular range of the FLC rotatable waveplates. In the context of this work, it is required to tune a null across the spectral band. This will occur when the birefringent element is halfwave in the region of the tuning band, or

$$\phi = (2m+1)\pi = \frac{2\pi \Delta nd}{\lambda}; \quad \text{m} = 1,2,3..... \tag{4}$$

where $\phi$ is the birefringence of the tuning stage including the optical thickness of the birefringent element and the applied phase of the QH cell and $\Delta$nd is the relative optical path difference for the o and e rays. From (4) it is evident that the separation between nulls at the $m^{th}$ and $(m+1)^{th}$ order is given by

$$S = \frac{2\ \phi\ \lambda}{(2m+3)(2m+1)} \qquad \text{from (4)}$$
$$= \frac{2\pi\lambda}{(2m+3)} \tag{5}$$

If the tuning range is given by $\Delta\lambda$, then the number of nulls in the tuning range is approximated by

$$N \approx \frac{\Delta\lambda(2m+3)}{2\pi\lambda} \tag{6}$$

where $\lambda_c$ is taken as the mid wavelength of the tuning range and the null wavelength. Equation 6 neglects dispersion and the increase in null spacing with wavelength but is approximately correct for arbitrary *m*. Taking the first derivative of Equation 4 gives

$$d\lambda = \frac{2\pi \Delta nd}{\phi^2} d\phi$$
$$= \frac{\lambda}{\phi} d\phi \tag{7}$$

which gives the tuning increment in the spectral null for an incremental change in phase. Combining Eqs (4), (6) and (7)

and integrating, the fraction of the spectral band Δλ which can be tuned for a change in birefringence $(\phi\text{-}\phi_o)$, is given by

$$F = \frac{(2m+3)}{(2m+1)} \frac{1}{2\pi^2} \int d\phi$$
$$= \frac{(2m+3)}{(2m+1)} \frac{1}{2\pi^2} (\phi - \phi_o) \tag{8}$$

From this result it is seen that the maximum tunable fraction occurs for a zero order birefringent element.

## 2.2 Binary Filter Design

The binary filters investigated exploit the switching properties of the smectic FLC cell specifically designed to act as a 90º polarization rotator at the design wavelength. Unlike the analog filters described previously, the binary filters employ two independent filter stages separated by an intervening polarizer with an active FLC device and passive elements in each stage. The conceptual operation of these filters is straightforward. Each filter stage comprised of a retarder stack between polarizers, is engineered to transmit a complimentary spectral profile. Switching between these profiles

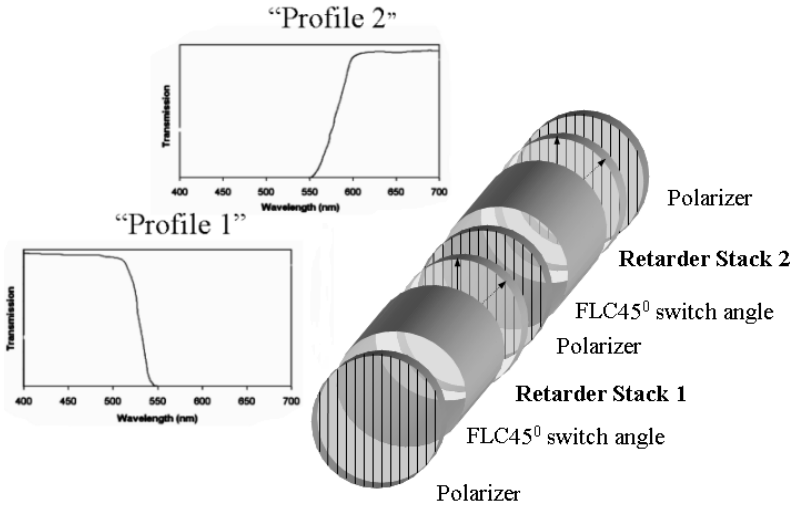


**Figure 4** Basic structure of the binary filters described in the text.

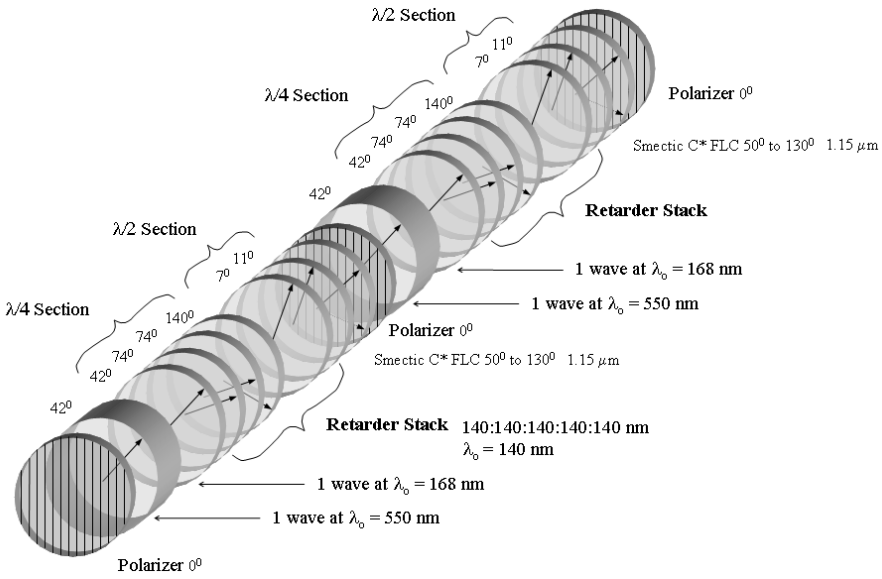


**Figure 5** Double stage visible analog tunable filter .

is accomplished with the smectic FLC cells, each of which is halfwave at the center of the spectral range. Referring to Figure 4, when "profile 1" is transmitted, the optic axis of FLC1 is oriented parallel to the input polarizer and is invisible in the context of polarization interference. In contrast the optic axis of FLC 2 is switched through $45^0$ so that a polarization rotation of $90^0$ occurs at the design wavelength. Stage 1 transmits its design profile while stage 2 transmits the compliment of its design profile which is a transmission window for stage 1 since the spectral profiles are complimentary. In this mode "profile 1" is transmitted. By the same argument, reversing the polarity of each FLC device transmits "profile 2". By using the above scheme it is possible to rapidly dither between complimentary states to generate a "white light" state, to block both states to produce a "black state" and to switch from one compliment to the other when unwanted radiation falls in a particular spectral region.

The main consideration in the design of binary filters lies in the development of retarder stacks which transmit complimentary spectral profiles with minimal spectral overlap. In designing these retarder stacks the method of Harris and Chang[11] was employed which shows that a sequence of birefringent elements can be treated as a Fourier series in the frequency domain with the Fourier components relating directly to the angular position of the fast axes of the birefringent layers. Using this method various waveforms such as a triangular or square waveform can be synthesized by stacking a sequence of NRF retarder sheets in the correct angular orientation.

## 3 RESULTS and DISCUSSION

### 3.1 Analog Filters

Figure 5 shows the construction of an analog filter designed for operation in the visible spectrum. The filter was constructed by combining layers of adhesive backed NRF retarder sheet at the appropriate angular orientation using an optical rotation stage. The retarder stack and FLC cell in each stage were aligned in an ANDO AQ-6315A spectrum analyzer by comparing the measured with the modeled spectrum and optimizing for maximum OD (given by

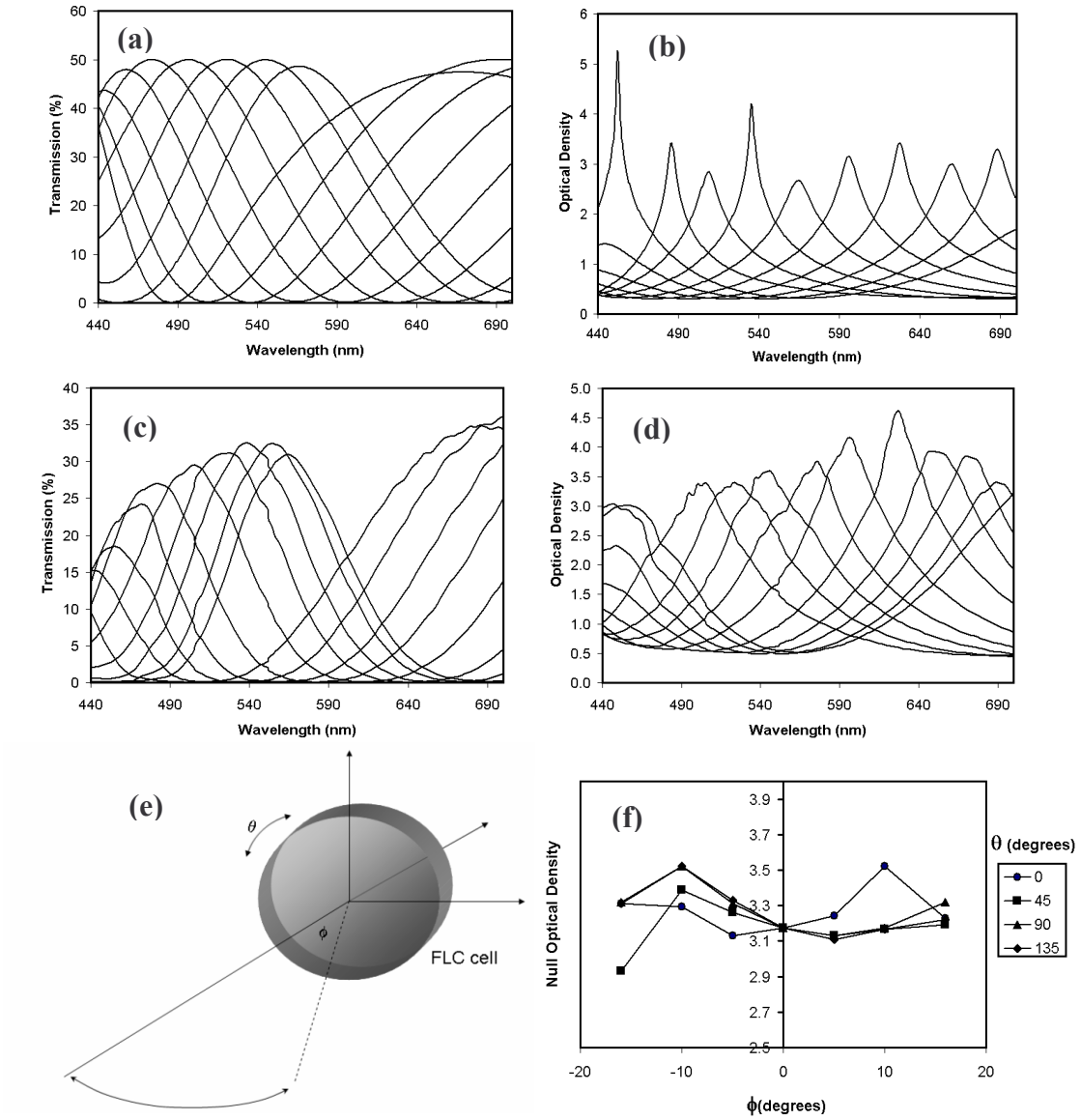


**Figure 6** Transmission characteristics of the analog filter detailed in Figure 5: (a) modeled transmission spectra for unpolarized light, (b) modeled optical density, (c) measured transmission spectra for unpolarized light, (d) measured optical density, (e) off-axis measurement geometry (f) off-axis measurement of the null optical density at 530 nm.

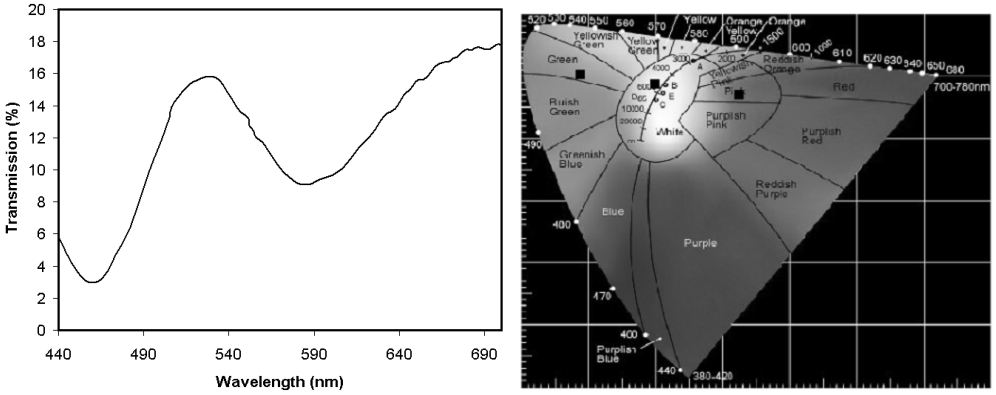


**Figure 7** "Pseudo white-light" state of the 440 nm – 700 nm analog filter, obtained by rapid dithering between complimentary spectral states. Chromaticity plot shows the complimentary states and resulting "white" state.

$Log_{10}$(output transmission/input transmission)). High throughput antireflection coated dichroic polarizers from Nitto Denko Inc. were then affixed as shown in Figure 5.

The filter is a 1st order filter with a 260 nm spectral tuning and employs two identical stages with a single high tilt FLC device. It is possible also to construct the second stage to yield twice the birefringence of the first in the standard Lyot-Ohmann filter geometry although this is not simply a case of doubling the optical thickness of the birefringent element in the second stage. Dispersion in the NRF material and the FLC devices, coupled with the non standard filter geometry designed to maximize OD, requires significant modeling and investigation into the optimal configuration for a second stage. This applies generally to all analog filters in the present kind. The spectral transmission characteristics of the above filter, recorded with an ANDO spectrum analyzer, are shown in Figure 6. The entire tuning range shown is accessed by varying the FLC voltage through 28 V, which tunes the LC director through its entire angular range. It is noteworthy that the modeled OD is significantly higher than that observed in the constructed device suggesting that the filter can be optimized further. This could be achieved by applying a more critical alignment technique for NRF elements in addition to an exact characterization of the optic axis direction in each individual layer. Nevertheless the measured OD across the tuning range is consistently above 3 which is relatively strong. The present filter is insensitive to off-axis degradation in the θ-ϕ region analyzed (Figure 6(c)).The angular position of the null did not vary significantly and the OD at the null remained close to 3.0. Further work is required to properly understand the off-axis performance of these filters. Finally the filter can operate in a pseudo "white light" state by rapidly dithering between two spectral states with roughly complimentary spectral profiles (Figure 7).

A second analog filter constructed for operation in the NIR (650 nm -910 nm) with a 260 nm tuning range is shown in Figure 8. A voltage change of 4.5 V is required to span the tuning range in this case, which switches the LC director through half of its angular range. In may be possible to design an NIR filter stage of higher order which exploits the full tuning range of the LC director and maintains the same spectral tuning width and this requires further analysis. Apart from the operating region, the operating principle is the same as in the case of the previous filter. In this case the filter is a zero order device with broadband spectra and wide nulls. Since the filter operates in the NIR, wire grid polarizers from Moxtek Inc were employed for this spectral region. Unfortunately these polarizers, as they are non absorbing, generate some leakage due to Fresnel reflections, thus reducing the OD at the nulls. Appropriate angular positioning of the polarizers can reduce this somewhat and eject the parasitic light out of the optical path. The off-axis performance of this filter is inferior to the previous case, possibly resulting from the fact that the NIR device employs a single stage only. In the case of the visible filter the two stages may have acted to compensate each other given that the stacks in each stage may be oriented in an orthogonal sense, although the filter was not deliberately constructed in this manner. The NIR filter can be dithered in a "white light" state in the same manner as with the visible filter. Figure 9 shows the transmission characteristics of the filter. Off-axis behavior is plotted in terms of the shift in the null which is significant in this case. Considerable leakage is also incurred at the null for off-axis viewing.

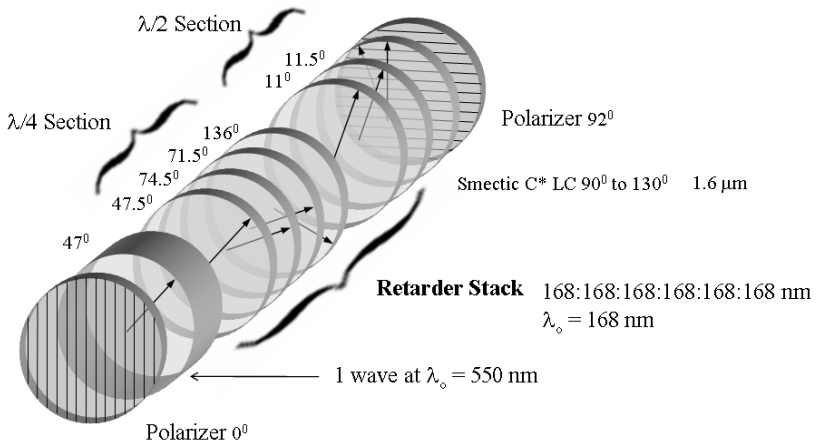


**Figure 8** Single stage NIR analog tunable filter

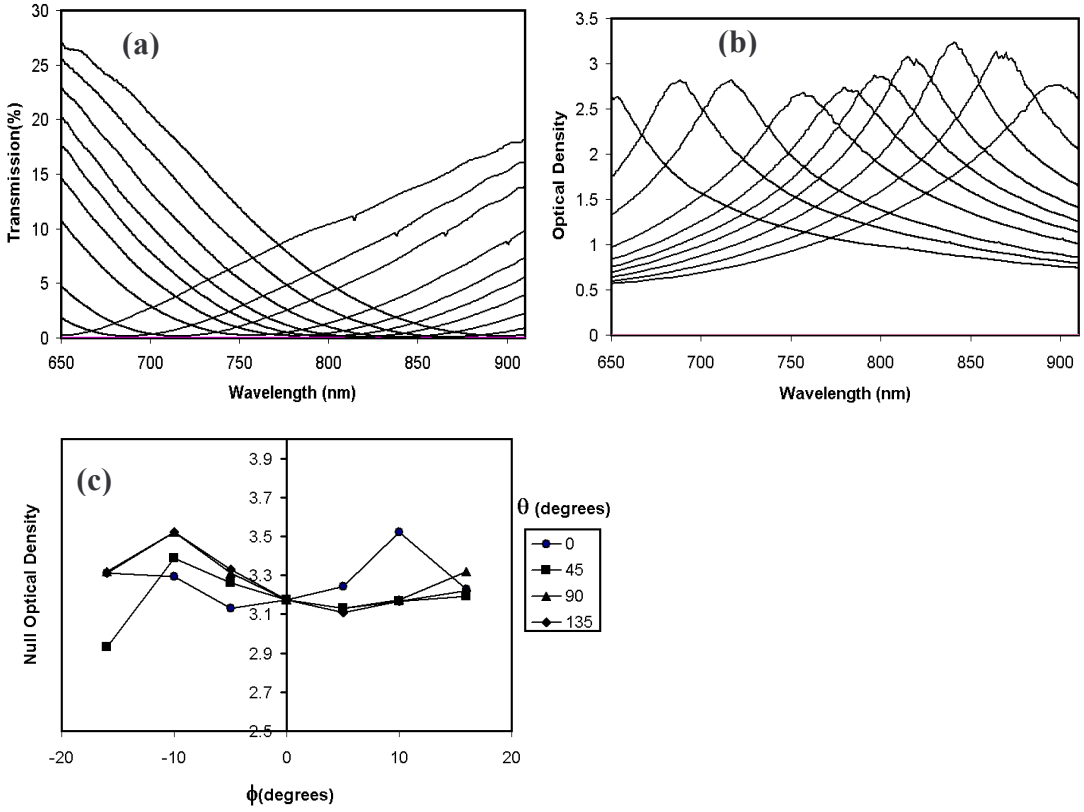


**Figure 9** Transmission characteristics of the NIR analog filter; (a) transmitted spectra for unpolarized light, (b) optical density plots, (c) off axis null shift.

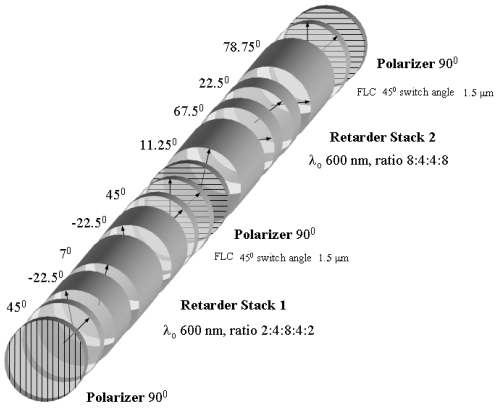


**Figure 10** Construction of the visible "comb filter".

### 3.2 Binary Filters

In the binary devices constructed, a liquid crystal compound which provided a 45º switching angle was chosen to provide ideal rotatable halfwave plates in the centre of the spectral band of the corresponding filter stage. Throughput was significantly lower in these devices as compared to the analog filters because of increased design complexity involving more retarder sheets and the requirement for dual stage operation. On the other hand the increase in passive elements yielded higher spectral definition

A filter referred to as a "comb filter" was constructed as shown in Figure 10. It operates on the principle of two spectrally separated interleaving comb functions associated with a particular stage of the filter. An ideal filter of this type would transmit a sufficiently high density of "comb peaks" in each state to maintain a broadband "white light" throughput in all circumstances. Blocking out unwanted radiation is then a matter of switching between combs without any perceivable change in transmission. In practice, however, achieving this level of performance would require a prohibitively large number of retarder sheets in each stack resulting in unacceptably degraded imaging. The number of retarder sheets used in the filter demonstrated is already considerable. The thicker sections of Figure 10 are built from several layers and in total 44 sheets are used to build this filter over the two stages. Each stage of the filter presented is constructed around a modified Solc filter geometry described elsewhere[12] which requires fewer elements than a standard Solc filter and is less subject to retarder misorientation errors..

Figure 11 shows the transmission characteristics of the comb filter. In addition to the interleaving comb states shown there are two other states corresponding to the two other switching combinations of the FLC's in addition to the dithered state. In the "black" state both stages are open simultaneously, and being complementary, each spectral function blocks the other with no net transmission. In the "white state" the combination of both comb states is transmitted as the FLC's produce the appropriate polarization rotation to sample the combined transmission functions of both stages. The modeled plots, generated with switching FLC devices and dichroic polarizers, predict a greater transmission than that actually measured. The losses in the constructed device are principally due to absorption and scatter in the NRF sheets which is significant due to the number of layers used. The construction of the filters could be improved by using higher order NRF material to replace a stack of lower order sheets. This would decrease the error in the relative angular orientation of sheets and improve the quality of the transmitted image by reducing the number of layer interfaces which cause distortion. Comb filters of the type described, but with reduced numbers of retarder sheets, can also be constructed at the cost of introducing spectral overlap between complimentary states at the tails of the transmission peaks.

In the ideal case, the filter would exhibit identical chromaticity for both comb states, however, the present results show that the filter switches between orange and green states of low saturation. The dithered state has essentially no color

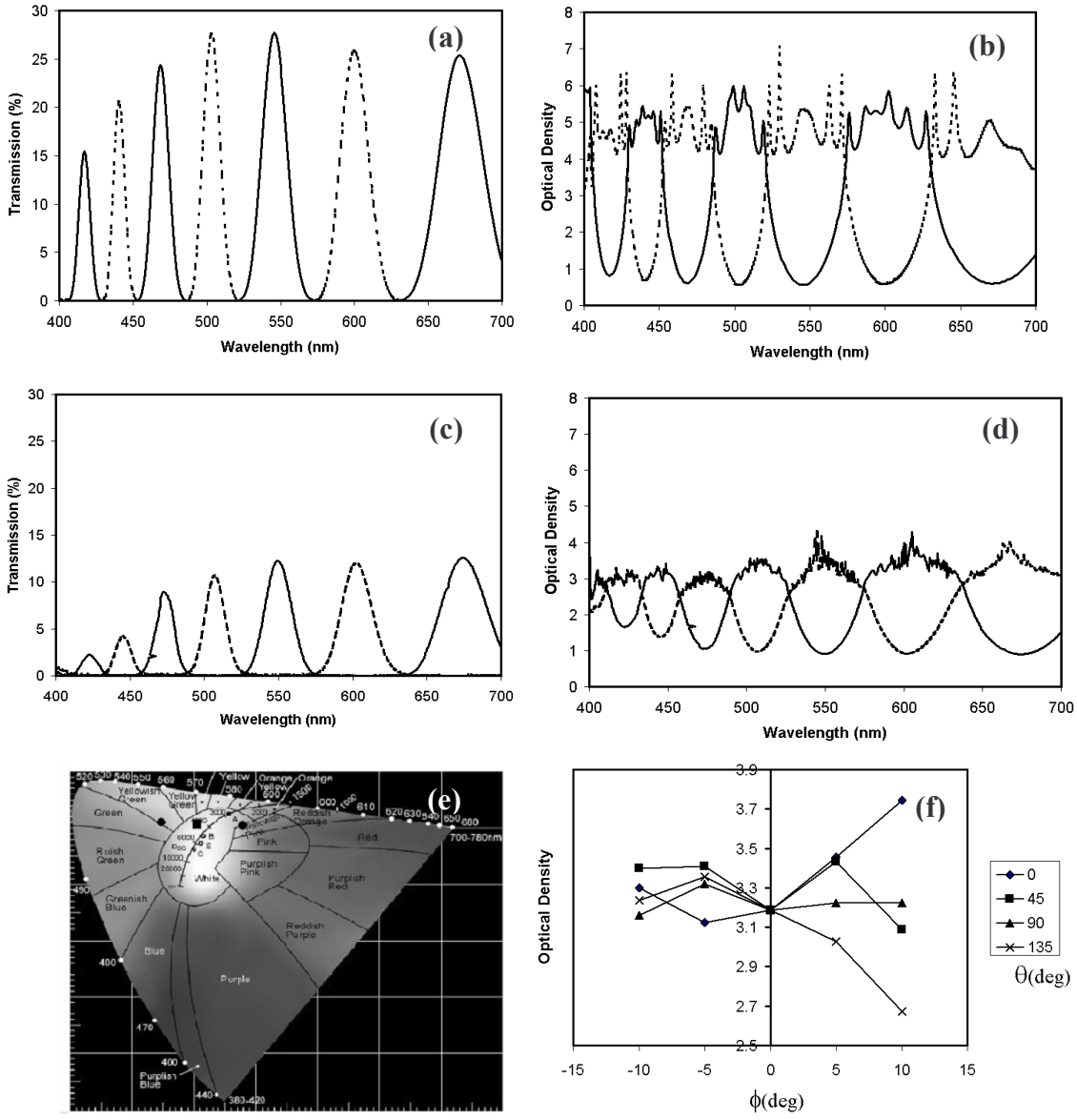


**Figure 11** Transmission states and optical density plots of the comb filter for unpolarized input; (a) and (b) modeled spectra, (c) and (d) measured spectra, (e) chromaticity points for the two comb states and for the dithered state, (f) off-axis optical density at the 550 nm null in one of the comb states.

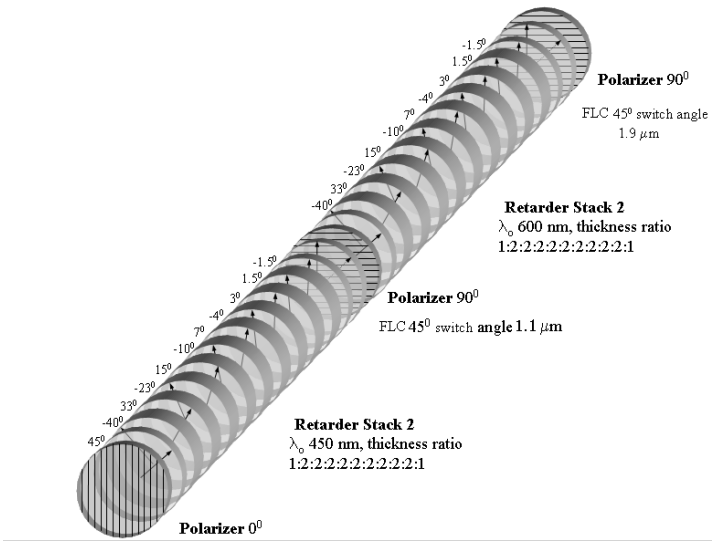


**Figure 12** Construction of the "half-switch" filter

saturation. The filter optical density in the stop bands is seen to vary between 3 and 4. Improvements to this can be expected if the filter construction is simplified and applied with greater precision. The off-axis data shown is typical for this type of filter with large retarder stacks; the OD is seen to vary between 2.7 and 3.7 in the θ-ϕ region examined although the null position remained essentially fixed.

A second type of binary filter, a so called "half-switch" filter was also constructed using the double stage geometry shown in Figure 10 but with interchanging spectral halves instead of combs. The construction of this filter required the fabrication of retarder stacks with a square wave transmission profile but displaced the appropriate amount in each case to yield non-overlapping states. The filter construction is shown in Figure 12 and the transmission characteristics in Figure 13. The peak transmission is superior to the comb filter, as is the overall wavelength integrated transmission in each state which is a better measure of the perceived throughput of the filter. The drop-off in the blue is due to absorption by the dichroic polarizers.

## 4 CONCLUSION

We have demonstrated novel optical filters for visible and NIR operation which are designed to provide a high OD null anywhere in the tuning band. Using a novel liquid crystal compound in surface stabilized smectic C* cells, a double tilt angle of 80º is exploited to provide a 260 nm spectral tuning range in the visible and in the NIR for two different filters. Binary filters have also been demonstrated which can switch between complimentary spectral states by employing two filter stages with retarders stacks configured for transmission of the desired complimentary spectral functions, and binary FLC devices which act as switchable halfwave plates.

The analog filters exhibit acceptable optical throughput for polarization based devices and can be further optimized by using appropriate fabrication methods. The binary filters, on the other hand, suffer from low transmission due to the large number of layers built into the retarder stacks. Simplifications are proposed which would employ single retarder layers in place of a multilayer stack with identical component orientation, and by sacrificing some spectral definition to reduce the number of layers used.

Modeling efforts predicted high OD's, up to 6 in some cases, for the filters designed. Measured OD's were more in the region of 3. Improvements to this are predicted with more precise fabrication procedures and material characterization.

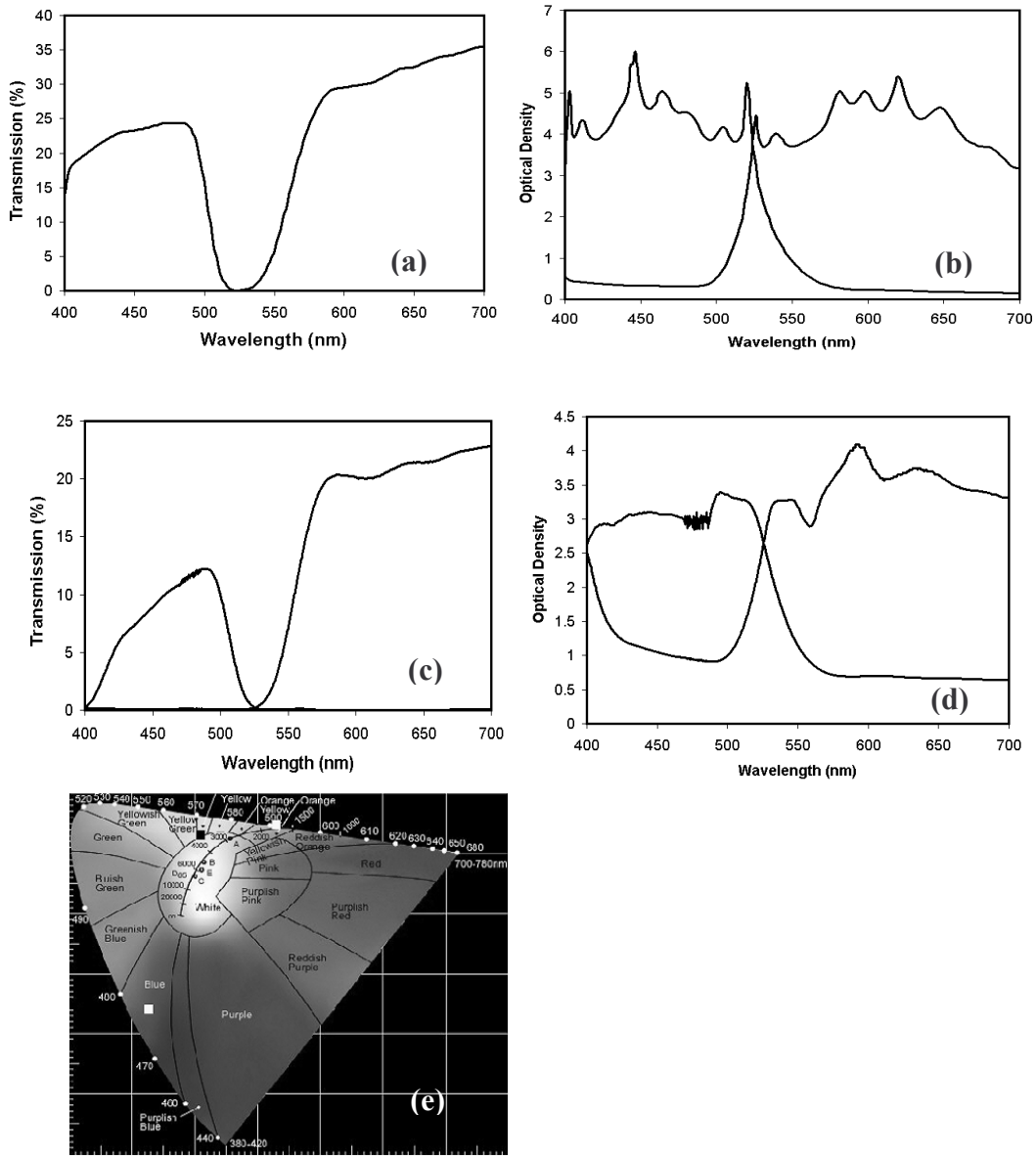


**Figure 13** Transmission states and optical density plots of the half-switch filter for unpolarized input; (a) and (b) modeled spectra, (c) and (d) measured spectra, (e) chromaticity points for the two spectral states and for the dithered state.

## 5 REFERENCES


[1] A. M. Title, W. J. Rosenberg, "Tunable Birefringent Filters", Opt. Eng., **20**, 815, 1981
[2] N. Gat, Proc. SPIE, **4056**, 50, 2000
[3] B. Lyot, "Optical Apparatus With Wide-Field Using Interference of Polarized Light", C.R. Acad. Sci., Paris, **197**, 1593 (1933).
[4] Pochi Yeh, "Optical Waves in Layered Media" (New York: John Wiley & Sons, Inc., 1988), 254.
[5] Shin-Tson Wu and Deng-Ke Yang, "Reflective Liquid Crystal Displays" (Wiley Inc. West Sussex , England, 2001),
[6] N. A. Clark, and S. T. Lagerwall, *Appl. Phys. Lett*. **36**, 899-901, (1980).
[7] A. M. Title, W. J. Rosenberg, Opt. Eng., **20**, 815 1981
[8] S. Pancharatnam, Raman Research Insitiute Bangalore, **71**, 137 (1955)
[9] G. Sharp, PH.D. Thesis, University of Colorado Boulder, 1992
[10]Charles J. Koester, "Achromatic combinations of half-wave plates", *J. Opt. Soc. Am.,***49**, 303 (1959).
[11] S.E. Harris, E. O. Amman, I. C. Chang, Journal Opt. Soc. Amer., Vol 54, p1267 (1964)
[12] I. Solc, "Birefringent Chain Filters", J. Opt. Soc. Am., **55**, 621 (1965).